Advanced Materials in Optics, Electro-Optics
and Communication Technologies
P. Vincenzini (Editor)
© Techna Srl, 1995

AU-COLLOIDS CONTAINING OPTICAL ACTIVE WAVEGUIDES BY SOL-GEL PROCESSING AND (NONLINEAR) OPTICAL PROPERTIES

M. Mennig, U. Becker, M. Schmitt, H. Schmidt

Institut fuer neue Materialien gem. GmbH, Im Stadtwald, 66123 Saarbruecken, Germany

Optical waveguides based on Au-colloid containing ormocer film with particle size from 10 nm to 40 nm in diameter have been prepared by sol-gel technique. The particles exhibit spherical as well as nonspherical shapes. Nonlinear optical measurements show a $\chi^{(3)}$ of a value of.2.8 $*10^{-7}$ esu for the composite and $\chi_m^{(3)} = 2.6*10^{-6}$ esu for the Au-particles.

1. INTRODUCTION

The investigation of third order non-linear optical phenomena ($\chi^{(3)}$ - effects) caused by Au colloids in glassy matrices has gained increased interest in the last years. Au colloids in SiO_2 layers made by sol gel processing [1] show 10 times larger $\chi_m^{(3)}$ coefficients than Au particles incorporated in glasses by high concentration ion implantation[2], by RF sputtering[3] or melting[4]. For the sol-gel system[1] it has been assumed that the large $\chi^{(3)}$ is due to non equilibrium states of the sol-gel derived Au colloids, since equilibrium is obtained by annealing the composite coatings at about 1000 °C. Recently a new preparation route for Au colloids in an ormocer coating based on methacryloxypropyl trimethoxysilane (MPTS) has been found[5], where Au colloids are formed in a very quick low temperature process by UV and IR irradiation during the curing of the matrix. One can assume that this rapid process of colloid formation in a simultaneously "freezing" matrix could lead to Au colloids in non equilibrium states and therefore it is very interesting to measure the $\chi_m^{(3)}$ value of these particles. In this synthesis route an excess of stabilizing ligands was used. In order to vary the particle size the ratio Au:ligand was varied. It was assumed that this ratio would affect nucleation and growth and this influence particle size and nonlinear properties. Since the capability for waveguide fabrication of the present Au containing sol-gel systems [1,5,12] is not proved yet, the second aim of this paper was to prepare Au colloids in an Ormocer matrix based on MPTS/ZrO_2 that has already

on MPTS/ZrO_2 that has already been used very successfully for the preparation of strip waveguides with buffer and cladding layers [6] and optical elements as gratings [7] and micro Fresnel lenses [7a].

2. EXPERIMENTAL

2.1 SYNTHESIS

To perform the synthesis of the Ormocer sol with the capability outlined in the introduction a prehydrolysed solution from 1 mole $CH_2=C(CH_3)-COO-(CH_2)_3-Si(OCH_3)_3$ and 1.5 mole 0.1 m HCl was added to 0.2 mole of an equimolar mixture of $Zr(OC_3H_7)_4$ and methacrylic acid and stirred for 4 h at room temperature. Finally 0.3 mole H_2O were added and the sol was stirred for 10 h.

900 mg $HAuCl_4 \cdot 3H_2O$ were dissolved in 9 ml of a mixture of ethanol, isopropanol and acetone (volume ratio 5:4:1). 0.5 ml of the silane $NH_2(CH_2)_2NH(CH_2)_3Si(OR)_3$ (DIAMO) were added to this alcoholic Au solution and then it was mixed with 20 ml of the Ormocer sol and again stirred for 4 h at room temperature. Finally a photocatalyst was added to the slight yellow sol to start the organic network formation during UV-radiation. Microscopy slides were coated by dipping with withdrawal speed of 1.5 mm/s. The curing of the films and the colloid formation reaction was induced using a Beltron UV-IR machine with a low pressure Hg-Xe lamp (polychromatic irradiation, 1500 W) and thermal radiation. The procedure takes about 1 minute and was repeated twice.

2.2 CHARACTERIZATION

To proceed the characterization optical absorption spectra of the coated slides were measured with an OMEGA 30 UV-VIS spectrometer (Bruins Instruments), the colloid sizes were determined using a JEOL 200 CX TEM and the thickness of the film was measured with a profilometer (diamont stylus, Nano-Surf). The $\chi^{(3)}$ was measured using the laser-induced grating (LIG) technique [8 9] in the selfdiffraction set-up. In this technique, also called forward degenerate four wave mixing (forward DFWM), two pump beams I_+ and I_- of equal frequency ω_{pump}, interfere with an angle θ

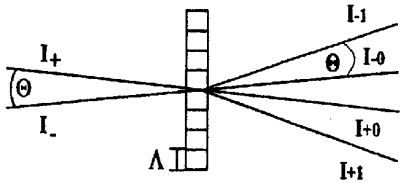

fig. 1: schematic picture of the LIG set-up

on the sample and diffract the probe beam at the induced grating. In the selfdiffraction configuration the probe beam is identical with one pump beam ($\omega_{pump} = \omega_{probe}$). The ratio between the transmitted beam and the first diffracted order intensities I_0/I_1 is called the diffraction efficiency η and determines the $\chi^{(3)}$ [9, 10] via eq. (1). The excitation energy of I_p was chosen to be in the maximum of the plasmon resonance.

$$^{(3)} = \frac{8n^2c^2\varepsilon_0\alpha\sqrt{\eta}}{3\omega I_p(1-T)\sqrt{T}} \qquad (1)$$

n= refractive index
c= speed of light
α= linear absorption
ω= frequency of I_p
I_p= pump intensity
T= transmission an I_p

The angle θ determines the grating constant $\Lambda=\lambda/(2\sin(\theta/2))$ of the induced grating. The light source was an excimer laser pumped dye laser which excited the sample with an wavelength λ_{exc}= 539 nm (2.3eV) on the peak maximum of the absorption. The pulse duration of the laser was 20 ns. The copolarized beams are focused to a spot of 160 µm diameter with an induced grating constant of 21 µm. The beams of one side of the diffraction pattern are directed to an 0.5 m spectrometer (Acton Research) coupled with a gated intensified CCD camera, where the beams I_{+0} and I_{+1} are detected simultaneously. The excitation intensity was varied in the range of 200 kW/cm^2 to 1 MW/cm^2.

3. RESULTS AND DISCUSSION

Following the outlined idea to use complexed Au-colloids in the synthesis route the waveguide formation and the resulting optical properties are discussed in this section. As complex ligand for Au^{3+} ions a diamino group containing silane according to [5] was chosen in a ratio of 1:1. A reaction process was developed, leading to the organic network formation and the thermal reduction of the ionic gold to Au^0 in a one step reaction. A photocatalyst activated by UV light initiates the organic network formation by photopolycondensation of the organic double bonds. At the same time the Au^{3+} in the films is reduced by the alcoholic compounds at temperatures <200 °C. It is assumed from investigations described elsewhere [11], that at low temperatures the DIAMO molecules used for the complexation of Au^{3+} remain attached to the formed Au colloids and thus form an interface to the matrix. Red coloured transparent crackfree films of 2 µm in thickness are obtained. WAXS investigations proof the crystallinity of the Au colloids and the crystallite size obtained by the method of Scherrer is about 8.5 nm in diameter. The TEM picture

(fig. 3) shows that the Au particles are spherical, spheroidal and some of them are of irregular shape. The particle size distribution determined from TEM is broad and ranges from about 10 nm to 40 nm in diameter. The formation of irregularly shaped particles has been observed in Pd systems with a Pd:DIAMO ratio ≤ 1:2 [14] as well as for Au colloids in Ormosils, prepared without any stabilizing ligand [12]. The mechanisms are not understood yet. One can consider an irregular growth or agglomeration effects caused by the uncomplete covering of the particle interface. This is in contrast to perfectly spherical Au colloids in lead silicate glasses obtained by long term heat treatment [13] or Pd [14] and Ag [15] colloids in sol-gel derived SiO_2 systems using sols with metal ions quantitatively bound to the DIAMO. The mechanism of this behaviour is still unknown and will be the subject of further investigations.

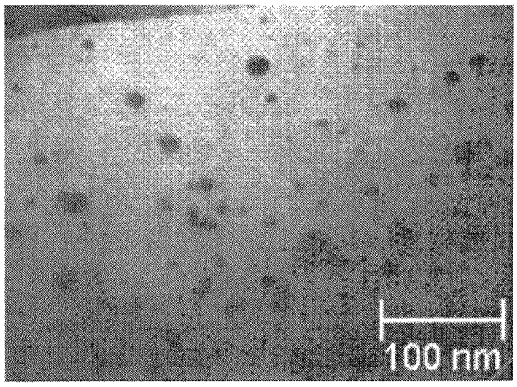

fig. 3: The TEM picture of the Au containing ormocer film

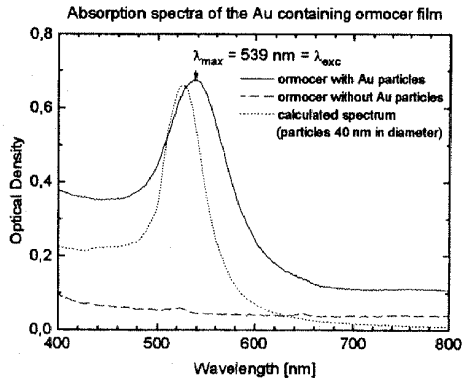

fig. 2: Absorption spectrum of a Au-containing ormocer film (d=4 µm). The long dashed line is the reference spectrum of the undoped ormocer, the short dashed line the theoretical value for the mean particle size in the sample.

The irregular shape of the Au colloids seems to have a remarkable influence on the linear optical properties. The UV-VIS spectra in fig. 2 shows the typical plasmon peak of Au-colloids at a wavelength around 539 nm (2,300 eV) with a full width at half maximum (FWHM) of 0.33eV (76 nm) and an optical density of 0.67. Even later than one year after sample preparation no change in the absorbance spectra was

observed (storing the samples at room temperature in a dark box). The dashed line represents the reference spectrum with the undoped ormocer (the peaks at 520 nm and 650 nm are artefacts) used for the determination of the absorption coefficient α of the Au colloid containing layer. The determination of the Au particle size using the peak position and the FWHM of the measured spectrum in comparison to calculated spectroscopic data based on the Mie-theory [13,16] leads to a diameter of about 50 nm. This value is much larger, compared to the results of the TEM investigation. This is not surprising, since non spherical Au colloids induce a broadening and a shift to longer wavelengths of the absorption band [13]. For confirmation the theoretical spectrum for spherical Au particles with a diameter of 40 nm (dotted line in fig. 2) is shown having an absorption of the plasmon band, which corresponds to the mean particle size in the ormocer discussed here. A shift of the maximum to 526 nm (2.357 eV) and a decrease of the FWHM to 52 nm (0.22eV) appears in contrast to the measured spectrum. From the area beneath the absorbance curve of the Au colloids (fig. 3) a volume fraction of colloidal gold in the Ormocer film of about 0.23 % was determined.

The LIG experiment showed a diffraction pattern to be observed visually on a screen, which vanished after one of the two pump beam was shut. In order to check, whether this was due to a real non-linear effect the grating efficiency η was measured as a function of the pump intensity. The result is given in fig. 4.

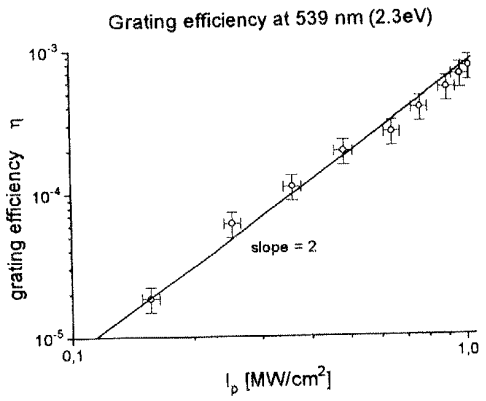

fig. 4: Grating efficiency η as a function of the pump intensity (λ = 539 nm) of the Au-colloid containing ormocer.

The grating efficiency increases quadratically in dependence of the pump intensity within the experimental errors, which is expected for a third order nonlinearity. The plotted line marks the slope 2. A reference sample without Au does not show any detectable third order nonlinearity under the same experimental conditions. To calculate the $\chi^{(3)}$ with equ. 1 the values n = 1.46 (approx. refractive index of the Ormocer), $\alpha = 3.6*10^5\ m^{-1}$ (Absorption deduced from fig. 2), T=0.23 (Transmittance of the pump light, taken from fig. 2, assumed to be independ-

ent of the I_p), c, ε_0, ω (velocity of light, dielectric constant and frequency of the exciting energy respectively) were used. The calculated $\chi^{(3)}$ values of the Au containing ormocer are depicted in fig. 5. The values are constant in the excitation intensity range. The averaged value of $\chi^{(3)}$ is $2.8*10^{-7}$ esu ($3.9*10^{-15}$ m^2/V^2). This is twice as high as the values in ion implanted and RF sputtered Au in glass[2,3] and two order of magnitudes higher than in melted glass[4]. The independence of $\chi^{(3)}$ from I_p indicates that no remarkable change of the absorption and no saturation effects occurs.

Since the measured $\chi^{(3)}$ is the effective value for the composite system, further calculation is performed to evaluate $\chi_m^{(3)}$, the non-linear third order coefficient of the Au colloids, following equations (2) and (3):

$$\chi^{(3)} = p f_l^2 |f_l|^2 \chi_m^{(3)} \qquad (2)$$

with

$$f_l = f_l(\omega) = \frac{3\varepsilon_d}{\varepsilon_m(\omega) + 2\varepsilon_d} \qquad (3)$$

with ε_d, ε_m = dielectric constant of the matrix and metal particles respectively, p= vol. fraction of the metal particles. Equ. 3 describes the internal field ratio between the matrix and the gold particles[17]. With the volume fraction p of 0.0023 and values for ε_m , interpolated from [18], $|\chi_m^{(3)}| = 2.6*10^{-6}$ is calculated. This value is two orders of magnitude higher compared to $|\chi_m^{(3)}|$ in melted[17] and ion implanted Au-composites[2] ($\chi_m^{(3)} = 4.8*10^{-8}$ for comparable particle size) and even one order of magnitude higher as the values of Matsuoka[1], obtained in a sol-gel silica glass composite.

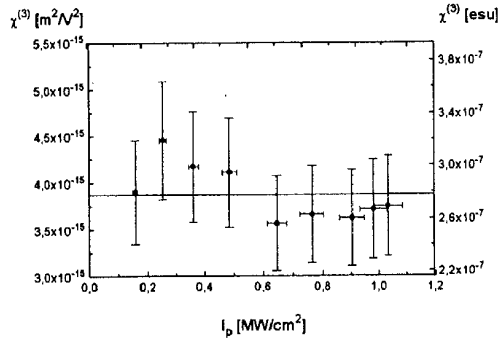

fig. 5: Non linear coefficient of the composit as a function of the pump intensity I_p in the DFWF experiment

Matsuoka observed a quick change of the absorption spectra during annealing the samples at 1000 °C which is interpreted as internal relaxation phenomena of the microstructure. Thus the system relaxes to a thermodynamically stable microstructure by heat treatment. Therefore it is assumed that the higher $\chi^{(3)}$ values result from the Au particles which are not in thermodynamical equilibrium. Since the sample discussed here exhibit

spherical and irregular shapes it is supposed that the simultaneous formation of the organic network and the Au colloids prevents the composite to reach real thermodynamical equilibrium. An influence of $\chi^{(3)}$ by particle agglomeration cannot be ruled out but refering to the TEM observation it is not concerning our results. It can also not be excluded that the electron donating ligands surrounding the particle in the interface to the matrix influence the electronic properties of the system and therefore can also contribute to the observed large $\chi_m^{(3)}$ values, because $\chi_m^{(3)}$ is due to the local field corrections in the composit. The nonlinearity in Au nano particles origins from the hot-electron contribution and from interband transitions but the dominating effect stems from the hot electron contribution. Even in the ns excitation time the hot electron contribution is the dominant one [17 and lit. cited therein]. To get a more comprehensive understanding of all the underlying processes further experiments have to be done in time resolved measurements, which include annealing experiments and a detailed analysis of the role of the matrix colloid interface.

4. CONCLUSION

The first approach to influence the particle shape of Au colloids in an ormocer matrix by using low complexation ratios resulted in spherical and irregular shaped Au particles in the matrix. The determination of $\chi^{(3)}$ effect shows values for $\chi_m^{(3)}$ two orders of magnitude higher than shown by colloids in a glass matrix. In the present understanding of the system the interface structure of Au-particles/ligands of the matrix enhances the nonlinear response. In comparison with the Au concentration to other methods (e.g. in ion implanted samples) a further increase of the nonlinearity can be expected since the processing allows to increase the Au content substantially. Further potential for investigation comprises the development of aspheric nano particles by ligand governed growth control.

ACKNOWLEDGEMENT

We thank Dr. Werner, who performed the TEM investigation of the film and the Ministry for Research and Culture of the State of Saarland for its financial support

1 J. Matsuoka, R. Mizutani, S. Kaneko, H. Nasu, K. Kamiya, K. Kadono, T. Sakaguchi, M. Miya, J. Cer. Soc. Jp, Int. Ed., **101** (1993) 55

2 K. Fukumi, A. Chayahara, K. Kadono, T. Sakaguchi, Y. Horino, M. Miya, J. Hayakawa, Jpn. J. Appl. Phys., 30 (1991) L742

3 K. Kadono, T. Sakaguchi, H. Wakabayashi, T. Fukumi, H. Yamanaka, M. Miya, H. Tanaka, Mat. Res. Soc. Symp. Proc. **283** (1993)

4 H. Hache, D. Ricard, C. Flytzanis, U. Kreibig, Appl. Phys. A **47** (1988) 347

5 L. Spanhel, E. Arpac, H. Schmidt, Proc. 6th. Int. Workshop on Glasses and Ceramics from Gel, ed. L. Esquivas, North Holland, 1991, 657 - 662

6 H. Krug, F. Tiefensee, P.W. Oliveira, H. Schmidt, SPIE- Proc. Sol-Gel Optics II, Vol. **1756** (1992), 448

7 H. Krug, H. Schmidt, Proc. American Ceramic Society meeting, Denver Colorado, March 28 - April 2, 1993, in print

7a H. Krug, H. Schmidt, Proc. 1. European Workshop on Hybrid Organic-Inorganic Materials, Chateau de Bierville France, Nov. 8.-10.1993, 127-142

8 H.J. Eichler, P. Günter, D.W. Pohl, „Laser-Induced Dynamic Gratings", Springer-Verlag Berlin, 1986

9 P. Horan, W. Blau, H. Byrne, P. Berglund, Appl. Opt. **29** (1990) 31

10 H. Hosono, Y. Abe, Y.L. Lee, T. Tokizaki, A. Nakamura, Appl. Phys. Lett. **61** (1992) 2747

11 M. Mennig, M. Schmitt, T. Burkhart, U.Becker, H. Schmidt, SPIE meeting Sol-Gel Optics III, San Diego 1994, to be published

12 J.Y. Tseng, C.Y. Li, T. Takada, C. Lechner, J.D. Mackenzie, Proc. of Sol-Gel Optics II (1992), SPIE Vol. **1758** (1992) 612

13 M. Mennig, M. Schmitt, H. Schmidt, K.-J. Berg, J. Porstendorfer: Proc. 2. ESG-Konferenz, Venedig 1993

14 T. Burkhart, M. Mennig, H. Schmidt, A. Licciulli: Proc. MRS Spring meeting San Francisco 1994, to be published

15 M. Schmitt, T. Burkhart, A. Kalleder, M. Mennig, H. Schmidt, 68. Glastechnische Tagung, Bad Salzdetfurth Germany, May 30 - June 1 1994, to be published

16 B. Dusemund, Master-Thesis, University Saarbrücken 1991

17 H. Hache, D. Ricard, C. Flytzanis, U. Kreibig, Appl. Phys. A **47** (1988) 347

18 P.B. Johnson, R.W. Christy, Phys. Rev. B **86** (1972) 4370